Magnetic field leakage of HTS medical accelerators

Magnetic Field Leakage of HTS Medical Accelerators

Yvonne T E Baird [1] and Quan Li [1]

[1] School of Engineering, Institute for Energy Systems, The University of Edinburgh, United Kingdom

Email: quan.li@ed.ac.uk

Abstract. A high temperature superconducting (HTS) magnet used in medical accelerators was designed with combined function for bending and focusing/defocusing, through a layer-by-layer design process. The six-layer combined function magnet produced by the layer-by-layer design process reduces the total volume of HTS material required compared to existing designs, in addition to achieving a precise field. The magnetic field distribution and leakage from the coil ends of the designed combined function magnet were studied, and the effects of changing the length of the coil ends as well as the radius of the layers were compared to the original design, to determine what influence this would have. Results show that shorter coil ends have the smallest leakage magnetic field, and is thus preferred, however due to mechanical constraints of HTS tape there will be a minimum length requirement depending on the design.

1. Introduction

Cancerous tumours can be treated using carbon-ion radiotherapy (CIRT), which offer a number of advantages compared to conventional treatment methods. Treatment is however limited to a few treatment facilities worldwide due to not only the costs associated with CIRT, but the size of the facility's accelerators and beam delivery systems [1]. The considerable size of the magnets and supporting structures are due to the large magnetic rigidity required to achieve the necessary kinetic energy of 430 MeV/u required for CIRT [2].

Existing HTS and LTS accelerator magnets have separated the dipole and quadrupole components by layers, which although is relatively straight forward to design, is not the optimal design when taking into consideration the quantity of superconducting material used for these designs. Unlike the previous designs, we propose a magnet which is designed with each layer generating both dipole and quadrupole functions for bending and focusing/defocusing of the beam respectively. The layers are generated layer-by-layer instead of simultaneously to use space more effectively. With this optimised design, further reduction of superconducting material is achieved allowing more compact magnets with precise magnetic fields.

This paper briefly describes the design of the combined function magnet and goes on to study the magnetic field distribution and leakage from the coil ends for the combined function magnets designed using the layer-by-layer algorithm. Altering the length of the coil ends in addition to changing the radius of the combined function layers is then studied, to determine the influence this has on the leakage magnetic field from the ends.

2. Designed combined function magnet

Unlike existing designs where the layers of the magnet are designed simultaneously, we apply an algorithm which designs the magnet layer-by-layer thus generating a magnet with layers designed individually [3]. The HTS combined function magnet is designed to achieve a dipole field of 2.88 T and a quadrupole field of 9.0 T/m, using a 5mm wide and 0.2 mm thick HTS tape. Additional design specifications are listed in table 1.

Table 1. Design specifications

Specification	Value	Unit
Radius of iron yoke	120	mm
Radius of mandrel	50	mm
Separation between coated conductors	0.1	mm
Coated conductor thickness	0.2	mm
Superconductor layer thickness	2	µm
Width of coated conductor	5	mm
Operation current	200	A
Magnet straight section length	1	m
Reference radius	35	mm
Higher harmonics	$<10^{-4}$	-
Flat-wise bending radius	>20	mm
Edge-wise bending strain	<0.3	%

The magnet was designed with left-right asymmetry in order to achieve the required bending and focusing/defocusing components. The flowchart for the steps to design the 2D cross-section of the combined function magnet is shown in figure 1 (a), whilst figure 1 (b) shows the cross-section design. The radius of the six individually designed layers are 50 mm, 57 mm, 64 mm, 71 mm, 78 mm, and 85 mm respectively. Generally a reference radius that is approximately 2/3 of the radius of the magnet is chosen for accelerator magnets, thus the reference radius was set at 35 mm [4].
An assumption was made that the current flows uniformly across the conductor width without any magnetisation current. In order to take into account the effect of the iron yoke the image current method was used [5], [6], [7].

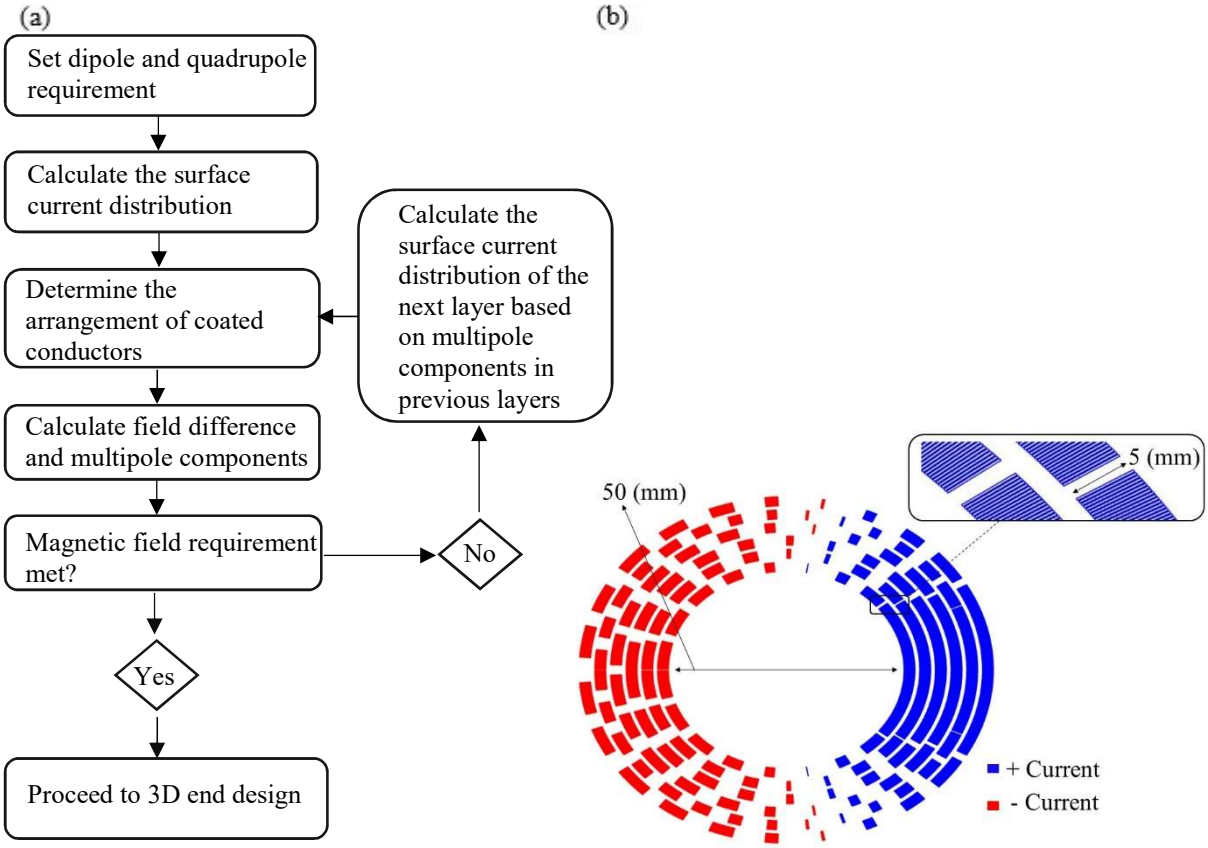

Figure 1. (a) 2D cross-section design flowchart; (b) new HTS layer-by-layer 2D cross-section design.

The coil ends were designed based on the cross-section design of the combined function magnet. Due to mechanical constraints of the HTS tape, edge-wise bending, flat-wise bending, and torsion was considered during the design by applying differential geometry [8], [9]. The results of the designed combined function magnet and the shapes of the coils for the six layers are shown in figure 2 and table 2. The total number of turns is 1259, while the total length of superconducting material is 6428.8 m. The higher multipole components normalised by the main dipole component were less than 10^{-4}, thus sufficiently small.

Table 2. Results for the designed combined function magnet

Parameter	Value	Unit
Number of turns		
Layer 1	336	-
Layer 2	370	-
Layer 3	404	-
Layer 4	450	-
Layer 5	456	-
Layer 6	502	-
Dipole field	2.93	T
Quadrupole field	9.05	T/m
Field uniformity	$<10^{-4}$	-
Conductor length		
Layer 1	816.4	m
Layer 2	903.6	m
Layer 3	1058.7	m
Layer 4	1147.7	m
Layer 5	1185.2	m
Layer 6	1312.2	m
Total length of coated conductor	6423.8	m

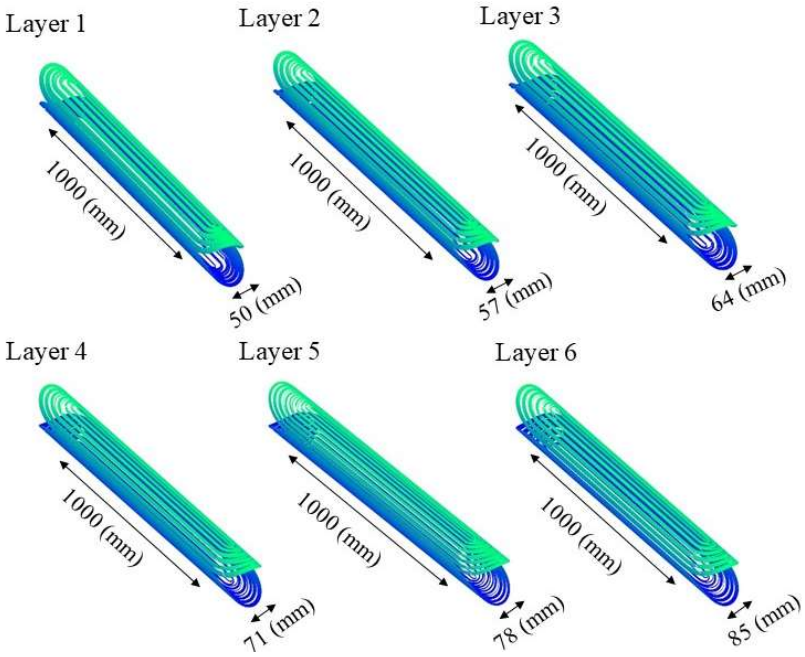

Figure 2. Shape of the six designed combined function layers, from first to last. Colour difference for clarity of design purposes only; darker blue colour showing the side of the coated conductors touching the mandrel. Note, the cylindrical mandrel is not shown. 1000 (mm) is the length of the straight section only.

3. Magnetic field distribution and leakage from coil ends

3.1. 50 mm mandrel combined function magnet

Figure 3 shows the magnetic field distribution for the combined function magnet with a 50 mm mandrel, and 35 mm reference radius. The colour plotting represents the magnetic field distribution for the six-layer combined function magnet from its centre to coil ends. The magnet straight section is 1 m long, hence the straight section in figure 3 is shown as the distance 0 mm to 500 mm, and the coil end region shown from 500 mm to 708 mm. From figure 3 it can be seen that the magnetic field design target of 2.88 T is achieved.

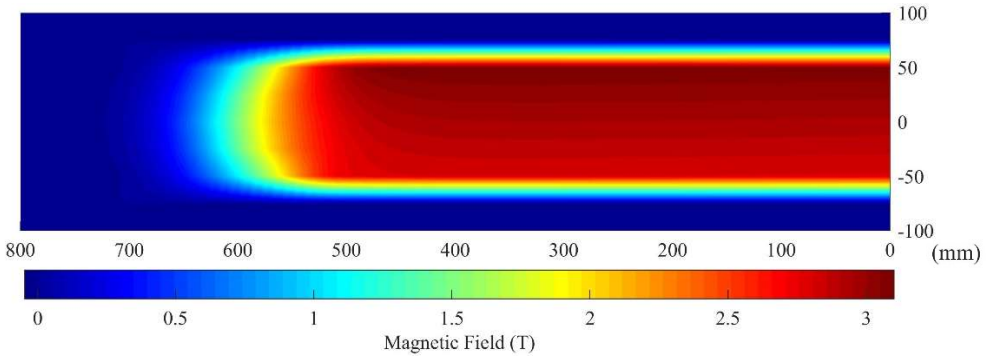

Figure 3. Magnetic field distribution for designed combined function magnet from its centre to coil ends.

The six layers of the combined function magnet coil ends is presented in figure 4 (a). The corresponding magnetic field distribution for the coil ends, as well as the leakage magnetic field from the ends is shown in figure 4 (b), with the outermost turn located at 708 mm.

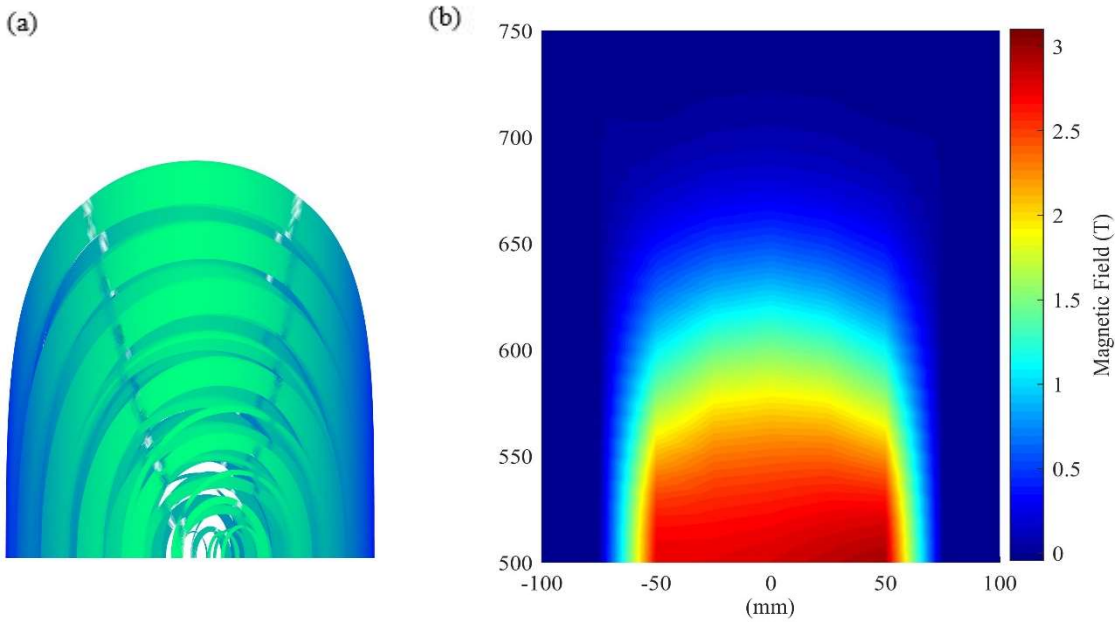

Figure 4: (a) Six layers coil ends, with colour difference for clarity of turns to avoid blending, (b) magnetic field distribution and leakage from coil ends.

Both the length of the coil ends as well as the radius of the layers of the combined function magnet were changed to determine what these effects would have on the leakage magnetic field, the latter of which is discussed in section 3.2. Figure 5 shows the change in magnetic field distribution and leakage magnetic field as a result of decreasing the length of the coil end by (a) 50 mm, and increasing the length of the coil ends by: (b) 50 mm, and (c) 200 mm. As expected, from figure 5 it can be seen that

as the length of the coil ends were increased the area of magnetic field distribution increased accordingly.

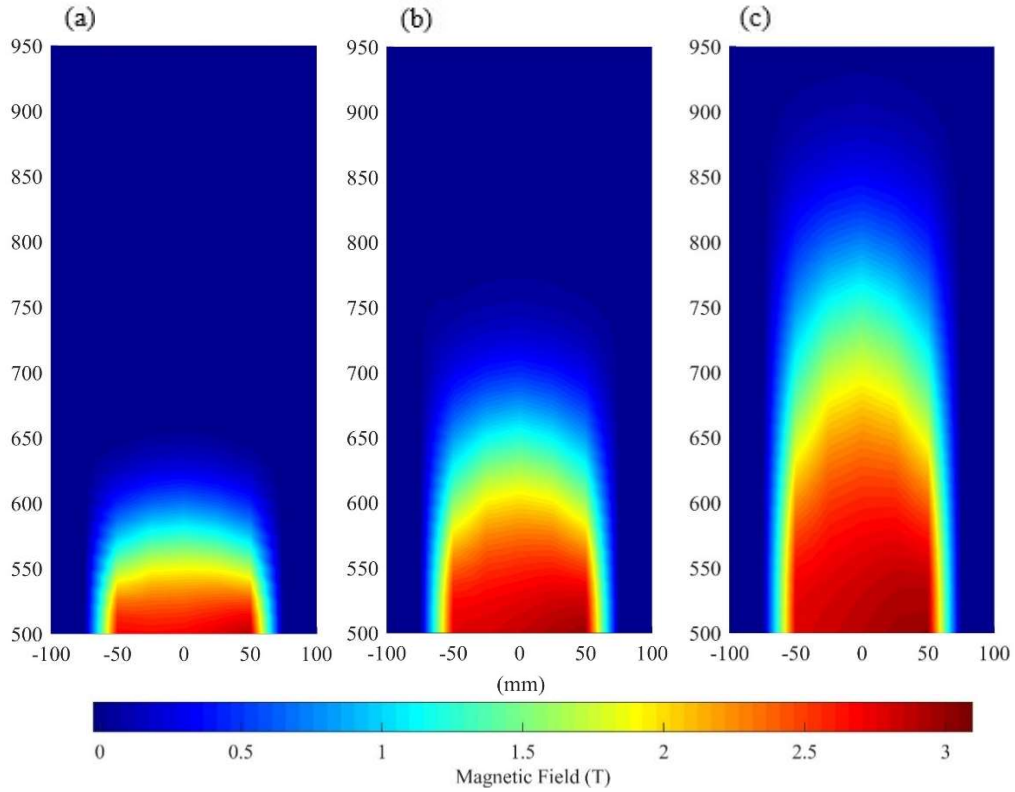

Figure 5. Magnetic field distribution and coil end leakage for the designed combined function magnet with length changed from original coil end length by: (a) 50 mm subtracted; (b) 50 mm added; (c) 200 mm added.

When taking a closer look at the leakage magnetic field from the ends a difference can be seen, as highlighted in figure 6.

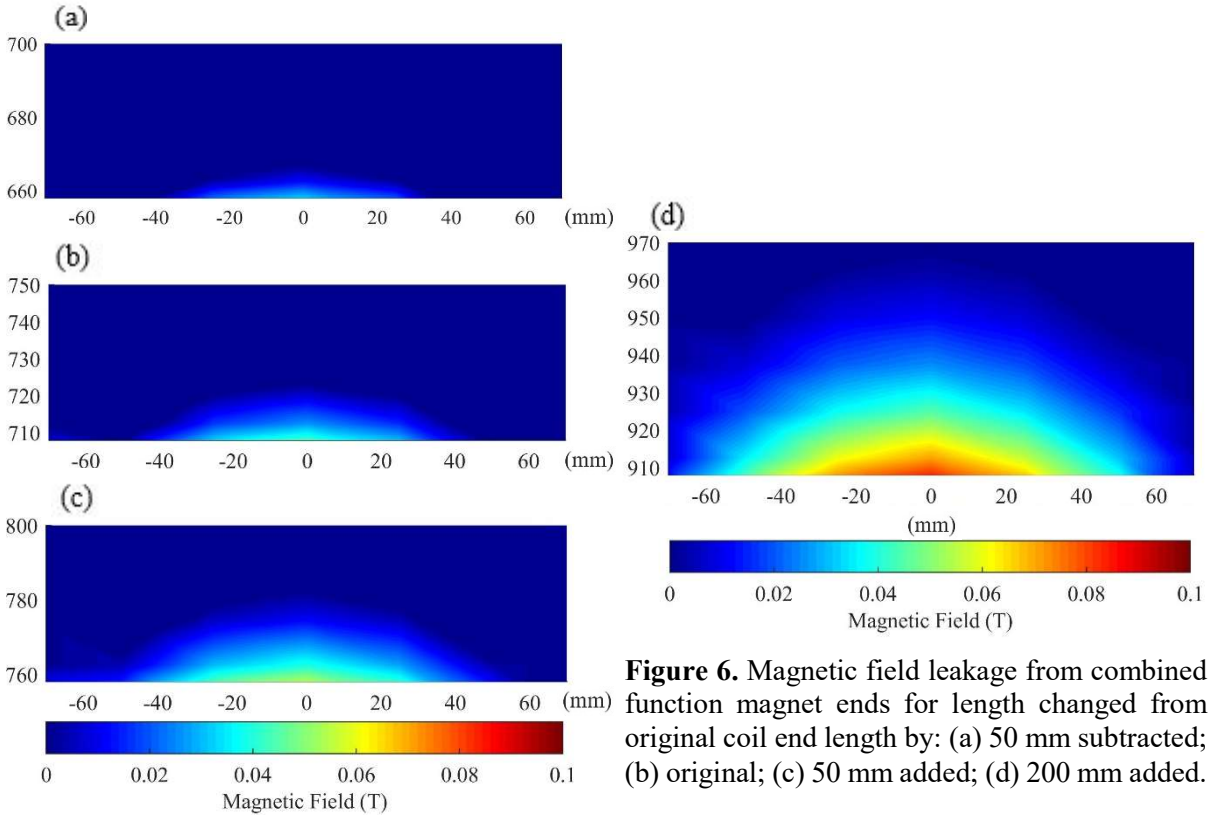

Figure 6. Magnetic field leakage from combined function magnet ends for length changed from original coil end length by: (a) 50 mm subtracted; (b) original; (c) 50 mm added; (d) 200 mm added.

The outermost turn for figure 6 (a) - (d) is located at length 658 mm, 708 mm, 758 mm, and 908 mm respectively. The figure shows that as the length of the coil ends increase the area of leakage magnetic field increases, in addition to the intensity. The intensity of leakage magnetic field after the outermost turn increased by 21.6 % as a result of changing the coil end length from 158 mm to 408 mm. This suggests shorter coil ends are preferred. However, the length of the coil ends have an impact on the edgewise bending strain, and must therefore also be considered. A shorter coil end is preferred to reduce coil end leakage magnetic field, but edgewise bending strain must not exceed 0.3 % [10], [11]. As seen from figure 7 (a) the edgewise bending strain for the innermost layer exceeds 0.3%, and affects a greater area of the tape compared to figure 7 (b). The innermost layer experiences the highest edgewise bending strain and was therefore chosen for the comparison. There is therefore a trade-off between reducing the leakage magnetic field, thus also volume of HTS tape used, and mechanical constraints of the HTS tape.

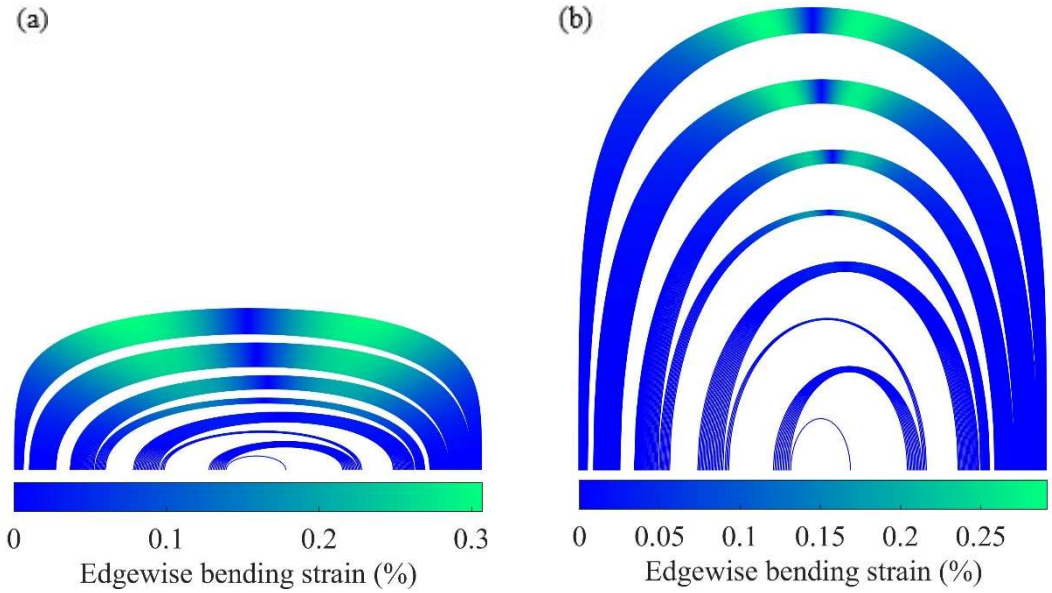

Figure 7. Edgewise bending strain for coil ends with length changed from original coil end length by: (a) 50 mm subtracted; (b) 200 mm added.

3.2. 60 mm mandrel combined function magnet

To determine whether the layers radius had an effect on the magnetic field leakage, the radius of the six layers were increased by 10 mm, thus the radius for the six layers were changed to 60 mm, 67 mm, 74 mm, 81 mm, 88 mm, and 95 mm respectively. Through changing the radius of the layers, a new combined function magnet was inevitably produced, with the half mandrel cross-section seen in figure 8 (a), and its corresponding coil ends in figure 8 (b). Although the 2D cross-section design and therefore the coil ends have changed compared to the design of the 50 mm mandrel, the length of the coil ends were kept constant.

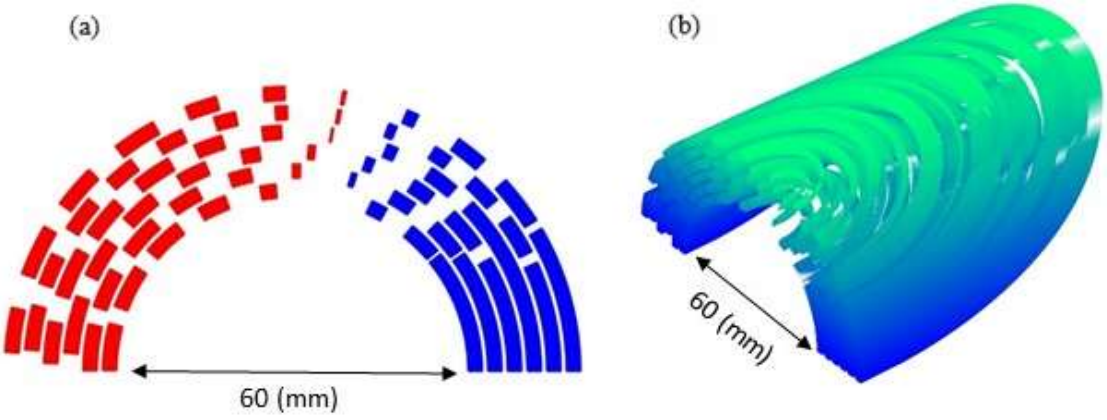

Figure 8. (a) 60 mm half mandrel combined function magnet design, (b) 60 mm mandrel combined function magnet coil end design, with colour difference for clarity of turns to avoid blending.

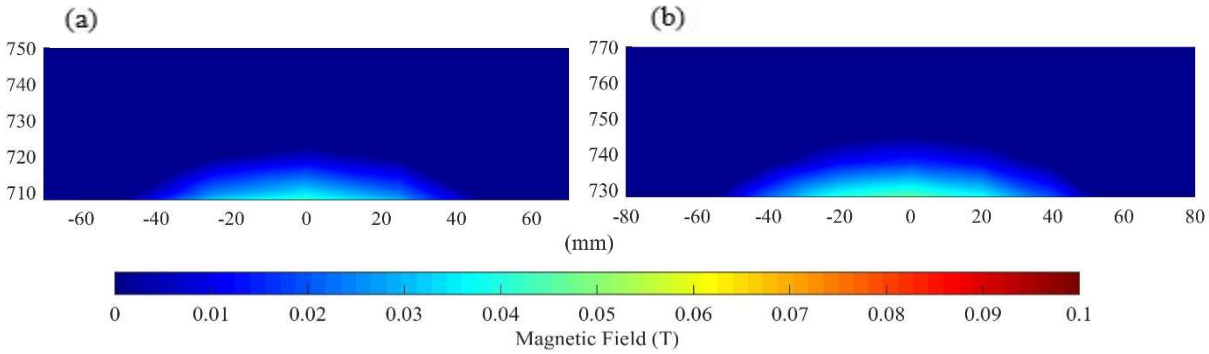

Figure 9. Leakage magnetic field for coil ends with mandrel of radius: (a) 50 mm; (b) 60 mm.

Figure 9 shows the comparison between the leakage magnetic field for the two designed combined function magnets, (a) a mandrel size of 50 mm, and (b) a mandrel size of 60 mm. As previously mentioned, the outermost turn for the 50 mm mandrel is at 708 mm in length, whereas for the larger mandrel of 60 mm the outermost turn is at 728 mm length. From the comparison a difference, although not considerable, can be seen. As the intensity of leakage magnetic field after the outermost turn remains constant at approximately 0.04 T before quickly reducing to zero, and only the area of leakage magnetic field increasing slightly, the small difference can be explained by the increased number of turns for the larger mandrel sized combined function magnet, needed to achieve the required dipole and quadrupole field components.

Although the edgewise bending strain for the innermost layer reduces when the mandrel size is increased to 60 mm as seen in figure 10 (b), the edgewise bending strain for the innermost layer with a mandrel size of 50 mm lies within the 0.3 % requirement as seen from figure 10 (a).

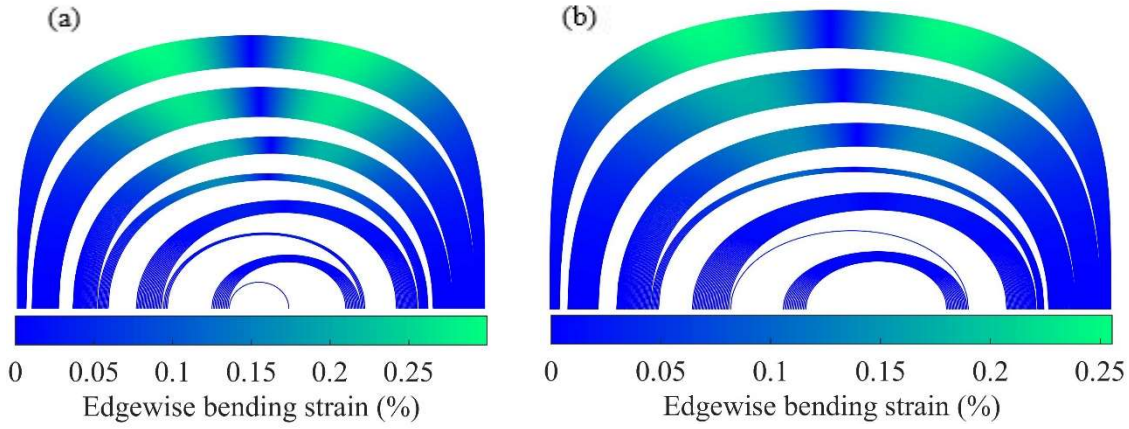

Figure 10. Edgewise bending strain for coil ends with mandrel of radius: (a) 50 mm; (b) 60 mm.

4. Conclusion

A combined function magnet was designed through a layer-by-layer design process to generate the required magnetic field, in addition to minimising HTS material use. The magnetic field distribution and leakage magnetic field from the coil ends of the designed combined function magnet were studied. The effect of changing the coil end lengths and radius of the layers were then presented. Changing the radius of the layers had a minimal influence on the leakage magnetic field, but reduced edgewise bending strain. A shorter coil end length is desirable as this has the smallest leakage magnetic field. An increase of 21.6 % was seen as a result of changing the coil end lengths from 158 mm to 408 mm.

However, due to mechanical constraints of the HTS tape, a minimum coil end length is required which depends on the design.

5. Acknowledgments

This work was supported by the Engineering and Physical Sciences Research Council [grant number EPSRC EP/M508032/1].

References

[1] Y. Iwata, T. Fujita, T. Fujimoto, T. Furukawa, Y. Hara, K. Kondo, K. Mizushima, T. Murakami, M. Muramatsu, M. Nishiuchi, E. Noda, K. Noda, H. Sakaki, N. Saotome, Y. Saraya and S, "Development of Carbon-Ion Radiotherapy Facilities at NIRS," *IEEE Transactions on Applied Superconductivity,* vol. 28, no. 3, April 2018.

[2] Y. Iwata, T. Shirai and K. Noda, "Design of Superconducting Magnets for a Compact Carbon Gantry," *IEEE Transactions on Applied Superconductivity,* vol. 26, no. 4, June 2016.

[3] Y. T. E. Baird and Q. Li, "Optimized Magnetic Design of Superconducting Magnets for Heavy Ion Ratating Gantries," *IEEE Transactions on Applied Superconductivity,* vol. 30, no. 2, 2020.

[4] S. Russenschuck, "Field Harmonics," in *Field Computation for Accelerator Magnets*, WILEY-VCH Verlag GmbH & Co., 2010, pp. 237-268.

[5] Y. Sogabe and N. Amemiya, "AC Loss Calculation of a Cosine-Theta Dipole Magnet Wound With Coated Conductors by 3D Modeling," *IEEE Transactions on Applied Superconductivity ,* vol. 28, no. 4, 2018.

[6] K. Takahashi, N. Amemiya, T. Nakamura, Y. Mori, T. Ogitsu, M. Yoshimoto, I. Watanabe and T. Yoshiyuki, "Magnetic Field Design of Coil-Dominated Magnets Wound With Coated Conductors," *IEEE Transactions on Applied Superconductivity,* vol. 22, no. 3, 2012.

[7] N. Amemiya, H. Miyahara, T. Ogitsu and T. Kurusu, "Design of a cosine-theta dipole magnet wound with coated conductors considering their deformation at coil ends during winding process," *Physics Procedia,* vol. 67, pp. 776-780, 2015.

[8] S. Russenschuck, "Differential Geometry Applied to Coil-End Design," in *Field Computation for Accelerator Magnets*, WILEY-VCH, 2010, pp. 609-636.

[9] B. Auchmann and S. Russenschuck, "Coil End Design for Superconducting Magnets Applying Differential Geometry Methods," *IEEE Transactions on Applied Superconductivity,* vol. 40, no. 2, 2004.

[10] D. v. d. Laan and J. W. Ekin, "Dependence of the critical current of YBa2Cu3O7−δ coated conductors on in-plane bending," *IOP Superconductor Science and Technology ,* vol. 21, no. 11, 2008.

[11] M.Sugano, K.Shikimachi, N.Hirano and S.Nagaya, "Simultaneously bending and tensile strain effect on critical current in YBCO coated conductors," *Physica C: Superconductivity and its Applications,* Vols. 463-465, pp. 742-746, 2007.